Journal of Molecular Catalysis A: Chemical 322 (2010) 80–89

Contents lists available at ScienceDirect

Journal of Molecular Catalysis A: Chemical

journal homepage: www.elsevier.com/locate/molcata

Co–Mo catalysts for ultra-deep HDS of diesel fuels prepared via synthesis of bimetallic surface compounds

Oleg V. Klimov*, Anastasiya V. Pashigreva*, Martin A. Fedotov, Dmitri I. Kochubey, Yuri A. Chesalov, Galina A. Bukhtiyarova, Alexandr S. Noskov

Boreskov Institute of Catalysis SB RAS, Novosibirsk, Russia

ARTICLE INFO

Article history:
Received 16 September 2009
Received in revised form 10 February 2010
Accepted 12 February 2010
Available online 19 February 2010

Keywords:
Hydrotreatment catalyst
Bimetallic Co–Mo oxidic precursor
Tetrameric molybdenum (VI) – citrate anion

ABSTRACT

The synthesis of bimetallic Co–Mo compounds from ammonium heptamolybdate, citric acid and cobalt acetate for the preparation of catalysts for the ultra-deep hydrodesulfurization (HDS) of diesel fuel is reported. The structure of the Co–Mo compounds formed in solution and on alumina surfaces was studied by ^{95}Mo, ^{17}O, ^{13}C, and ^{27}Al NMR, FTIR, Raman and XAS spectroscopy. It was found that the oxidic precursor of the catalyst consists of tetrameric molybdenum (VI) citrate anions with Co^{2+} cations coordinated to the carboxyl groups and terminal oxygen atoms. After sulfidation, the prepared catalyst was tested in the HDS of straight run gas oil, demonstrating high activity in the production of ultra-clean diesel fuel.

1. Introduction

In recent years, considerable work has been devoted to the preparation of hydrodesulfurization (HDS) catalysts using bimetallic Co(or Ni)–Mo compounds. Two general approaches are described in the literature: preparation with the heteropolyanions (HPA) initially consisting of both Co and Mo [1–5], and preparation of the bimetallic complexes in solution from Mo-containing HPA and cobalt (or nickel) cations [1,6,7]. According to Refs. [8,9], the most active HDS catalysts, regardless of the preparation process, have a ratio of cobalt load to total metal load between 0.3 and 0.6, i.e. a Co/Mo ratio within the 0.5–1.5 range. At this level, the bimetallic precursor of the catalyst should contain the same Co/Mo atomic ratio. However, the regular Co–Mo heteropolyanions with Keggin, Dawson or Anderson structures have Co/Mo ratios well below 0.5. For instance, 6-molybdocobaltate with an Anderson structure ($(NH_4)_3[CoMo_6O_{24}H_6]\cdot 7H_2O$) has a Co/Mo value of 0.17 [5,10]. To achieve the optimal level for HDS purposes, one thus needs to add extra Co^{2+} cations to the HPA solution, which results in the formation of the cobalt (II) salt of HPA [1–3,11]. In a similar fashion, cobalt salts have been synthesized from Co^{2+} and molybdenum-based anions [1,6,7]. The reported preparation processes do yield supported catalysts with better activity in the hydroconversion of thiophene as compared to catalysts prepared from the traditional precursors, i.e. ammonium heptamolybdate and cobalt nitrate. Some researchers think that the superior activity of these catalysts is due to the stability of the bimetallic Co–Mo complex synthesized in solution during its deposition on the alumina surface [1–3]. In this case, the formation of various cobalt compounds leading to compounds that are inactive in HDS is hindered [12].

However, close inspection of the EXAFS and Raman spectra shown in Refs. [1–3] allowed us to conclude that a considerable fraction of the original Co–Mo compound had lost its structure in the course of the deposition, most likely due to decomposition. The authors of Ref. [13] showed that the interaction of $H_2PMo_{11}CoO_{40}^{5-}$ with alumina occurs through the dissociation of HPA. When phosphomolybdate anions are used as precursors for alumina-supported catalysts, the formation of surface aluminum phosphates and the dissociation of phosphomolybdate anions occur due to local variations of basicity in the pores of the support [14,15]. Bimetallic compounds consisting of Co^{2+} coordinated to $Mo_7O_{24}^{6-}$ anions [6] or to $H_2P_2Mo_5O_{23}^{4-}$ [16] were found to decompose to form a variety of species because of the interaction with the alumina surface. In all of these cases, some cobalt atoms cover the alumina surface in such a way that they do not participate in the subsequent preparation stage. The formation of a Co–Mo–S Type II phase that causes an increase in the catalytic HDS activity is reported in Refs. [17,18].

* Corresponding authors at: Boreskov Institute of Catalysis SB RAS, pr. ak. Lavrentiev, 5, Novosibirsk, 630090, Russia. Tel.: +7 3833269410; fax: +7 3833308056.
E-mail addresses: klm@catalysis.ru (O.V. Klimov), pav@catalysis.ru (A.V. Pashigreva).

1381-1169/$ – see front matter © 2010 Elsevier B.V. All rights reserved.
doi:10.1016/j.molcata.2010.02.020

We previously reported the synthesis of highly active HDS catalysts using bimetallic Co–Mo compounds [19]. The following items were taken into account during this process:

- intentional synthesis of the bimetallic Co–Mo complex in aqueous solution with Co and Mo stoichiometry that is optimal for the hydrogenolysis of C–S bonds (i.e. Co/Mo = 0.5);
- implementation of the specific coordination of cobalt with molybdenum in the synthesized compound, providing a stable vicinal arrangement of Co and Mo in the subsequent synthesis stages to achieve the formation of homogeneous bimetallic sulfide compounds with the proper chemical composition, structure and particle size distribution for the catalysis of HDS reactions;
- in addition to cobalt and molybdenum, the complex compound included some ligands to promote proper Co coordination and to prevent the formation of poorly soluble bimetallic species and subsequent sedimentation;
- evaluation of safe conditions for the deposition of the primary bimetallic complex from solution to the alumina surface without disruption of its structure.

In the present paper, we report catalysts for the ultra-deep HDS of diesel fuels that contain a Co/Mo ratio of 0.5, bimetallic surface compounds on alumina as oxidic precursors of the active centers, and the preparation procedure based on the synthesis of bimetallic complexes in aqueous solution.

2. Experimental

2.1. Preparation of the complexes and catalysts

The bimetallic compound for catalyst preparation was synthesized from the ammonium salt of the tetrameric citrate anion $[Mo_4(C_6H_5O_7)_2O_{11}]^{4-}$, which was prepared via dissolution of 44.8 g (0.234 mol) of citric acid and 57.9 g (0.328 mol of Mo) of ammonium heptamolybdate $(NH_4)_6Mo_7O_{24}{\cdot}4H_2O$) in a small amount of distilled water, followed by the addition of more water to obtain exactly 200 ml of solution (hereafter denoted as (Mo_4citr-solution)). The 40% excess of citric acid over the stoichiometric ratio in the prepared solution is necessary for preventing sedimentation in the stock solution or during the impregnation of alumina. Moreover, the overbalanced citric acid provides the optimal pH (1.5–3.5) for the stability of the tetrameric complex, because at higher pH values, it decomposes to bi- and mononuclear Mo species [20–24].

The sample denoted as (Mo_4citr-solid) was prepared by stirring a mixture of 250 ml of ethanol and 50 ml of (Mo_4citr-solution) to get a white precipitate, which was then filtered, washed with ethanol and dried in a fume hood. The sample designated as (Mo_4citr/Al_2O_3) was obtained via the impregnation of alumina with (Mo_4citr-solution). The impregnation procedure was carried out with intermittent stirring of alumina granules in a solution volume that was 25% greater than the water sorption capacity of the 'dipped-in-support' granules. After 2 h of stirring, the supernatant was drained out and stocked (designated as Mo_4citr-solution AI) (after impregnation). The solid fraction was dried at room temperature. Some part of the (Mo_4citr/Al_2O_3) was then annealed for 4 h at 550 °C in air. Additional evaluation showed a Mo load of 11.5 wt.% for the calcined sample.

The same alumina support was employed for all of the samples, and this support was the product of ZAO "Industrial catalysts", Ryazan, Russia. This support has a specific surface area of 285 m^2/g, a pore volume of 0.82 sm^3/g, an average pore diameter of 115 Å and fractions of 0.25–0.5 mm.

The sample marked as (Co_2Mo_4citr-solution) was prepared by solubilization of solid $Co(CH_3COO)_2{\cdot}4H_2O$ in (Mo_4citr-solution) in proportions equivalent to a Mo/Co = 2 atomic ratio. The resulting solution, under ethanol precipitation (similar to Mo-only sample procedure described above), gave a rose-colored powder of (Co_2Mo_4citr-solid). Impregnation of alumina with (Co_2Mo_4citr-solution), followed by the room temperature drying procedure yielded the catalyst sample denoted (Co_2Mo_4citr/Al_2O_3), with metal loads of 11.2%Mo and 3.5%Co (in the calcined sample).

2.2. Complexes and catalyst characterization

2.2.1. NMR spectroscopy

NMR spectra at natural isotopic abundances were recorded in an AVANCE-400 Bruker spectrometer at frequencies of 26.06 (^{95}Mo), 100.4 (^{13}C), 54.24 (^{17}O) and 104.3 (^{27}Al) MHz with accumulation rates of 45, 0.1, 45 and 10 Hz, respectively. NMR spectra of ^{17}O were recoded at the natural isotope content during 2 h. The chemical shifts (in ppm) were referenced to external standards of H_2O (^{17}O), tetramethylsilane (^{13}C), and 2 M solutions of Na_2MoO_4 (^{95}Mo) and $Al(H_2O)_6^{3+}$.

The samples (Mo_4citr-solution) and (Mo_4citr-solution AI), as well as a comparison sample of 0.5 M citric acid, were evaluated. To investigate the coordination of Co cations with $[Mo_4(C_6H_5O_7)_2O_{11}]^{4-}$ anions, a series of solutions with Mo/Co ratios of 40, 20, 10, 5 and 2 were prepared by dissolving different amounts of solid $Co(CH_3COO)_2{\cdot}4H_2O$ in (Mo_4citr-solution).

2.2.2. Raman spectroscopy

Raman spectra were recorded at room temperature in the range of 3600–100 cm^{-1} using a Bruker RFS 100/S FT-Raman spectrometer (Germany). The excitation source used was the 1064 nm line of a Nd-YAG laser operating at power level of 100 mW.

2.2.3. FTIR spectroscopy

IR spectra were acquired in the range of 4000–250, with 4 cm^{-1} resolution in a Bomem MB-102 FTIR spectrometer. The solid specimens were generated via the conventional procedure, i.e. by the tableting 1.5 mg of the probe with 500 mg of KBr. The liquid aqueous specimens were placed inside a KRS-5 capillary cuvette. In this case, the recorded spectra were subtracted from the normalized spectra of distilled water at 700 cm^{-1} (the broad absorbance band of water molecule vibrational stretching).

2.2.4. XAS spectroscopy

The EXAFS spectra of the Mo–K and Co–K edges were obtained at the EXAFS Station of the Siberian Synchrotron Radiation Center (Novosibirsk), under the conventional transmission mode [25]. The storage ring VEPP-3, with an electron beam energy of 2 GeV and an average stored current of 100 mA, was used as the source of radiation. The spectrometer had a Si(1 1 1) cut-off crystal-monochromator and two proportional ionization chambers as detectors. The spectra were recoded at room temperature. For each sample, the oscillating piece of the EXAFS spectra ($\chi(k)$) was treated in the form of $k^2\chi(k)$ at the wave number interval of 2.5–14.0 $Å^{-1}$. The EXAFS spectra simulations for retrieving the structure data were performed by using the standard procedure with the VIPER code [26]. The FEFF7 program was employed to fit the parameters of scattering [27].

2.3. Sulfidation of the catalyst and testing in HDS

Sulfidation of 2 g of (Mo_4citr/Al_2O_3) and (Co_2Mo_4citr/Al_2O_3) was performed in an H_2S flow of 1000 ml h^{-1} at atmospheric pressure with ramping of the temperature from 20 to 400 °C over 1 h, followed by exposure to 400 °C for 2 h.

After sulfidation, the catalysts were tested in the hydrodesulfurization of straight run gas oil containing 1.05 wt.% S. The experiment

Table 1
^{95}Mo, ^{17}O and ^{13}C NMR data of aqueous solutions. The signals with intensivity less than 5% of the maximal signal are not included.

Sample	δ ^{95}Mo (W) [I]	δ ^{17}O (W)	δ ^{13}C
0.5 M $C_6H_8O_7$	–	261(460); 246(540)	177.8; 174.4; 74.3; 44.3
(Mo_4citr-solution)	76 (250)[0.05]; 36(360)[1.0]; −54(380)[0.67]	865(700); 830(1600); 371(600); 260(1300)	184.7; 182.1; 174.6; 173.9; 85.7; 43.7
(Mo_4citr-solution Al)	76 (230)[0.05]; 37(500)[1.0]; −53(560)[0.92]	867(750); 830(1300); 374(420); 263(1500)	184.5; 182.1; 174.1; 173.9; 85.7; 43.9
Mo/Co = 40	88 (280)[0.05]; 38(740)[1.0]; −48(790)[0.72]	870; 841; 373; 266 (1460)	187.3; 181.4; 179.0; 176.6; 89.1; 46.9
Mo/Co = 20	100 (390)[0.06]; 46(750)[1.0]; −34(800)[0.78]	874; 850; 373; 271(1300)	190.2; 183.3; 182.0; 178.8; 92.8; 49.1
Mo/Co = 10	99 (730)[0.13]; 57(780)[1.0]; −22(820)[0.92]	847; 372; 275(330)	195.0; 189.8; 186.8; 184.0; 100.7; 55.9
Mo/Co = 5	205 (920)[0.23]; 86(1360)[1.0]; 18(1250)[0.75]	376	212.3; 209.5; 202.3; 197.2;121.2; 63.4
Mo/Co = 2	90(1500); 40(1500)	–	No data

δ – chemical shift, ppm; W – width of a line, Hertz; I – intensity, relative units.
Underlined values, is not assigned to $[Mo_4(C_6H_5O_7)_2O_{11}]^{4-}$ anion.

was performed in a plug flow stainless steel reactor at 3.5 MPa with T = 320–360 °C, a liquid hourly space velocity of 1.5–4.0 and an H_2/feed volume ratio of 300. In such conditions, the weight liquid product output was 94–96%, mainly due to the efficiency of the apparatus separator.

The sulfur content in the liquid products was measured using a Horiba SLFA-20 X-Ray fluorescence analyzer.

3. Results

3.1. NMR analysis of the solutions

^{95}Mo, ^{17}O and ^{13}C NMR data for the samples (Mo_4citr-solution), (Mo_4citr-solution Al), 0.5 M citric acid and (Mo_4citr-solution) with different weights of cobalt acetate are compiled in Table 1. To better understand the chemical processes in solution, precise information on the broadening and peak shapes is displayed for the ^{17}O and ^{13}C spectra (see Figs. 1 and 2).

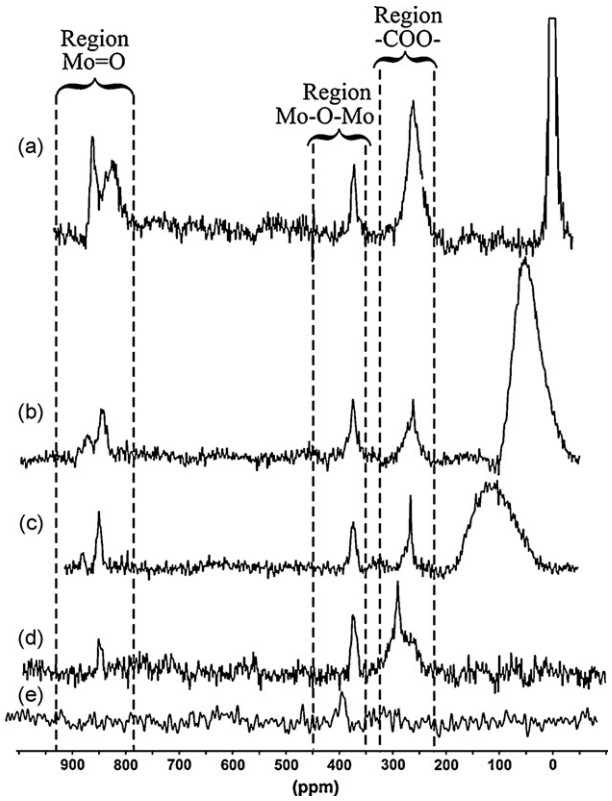

Fig. 1. ^{17}O NMR spectra of solutions. (Mo_4citr-solution) (a) and (Mo_4citr-solution) with different Co^{2+} addition: (b) Mo/Co ratio 40, (c) Mo/Co ratio 20, (d) Mo/Co ratio 10 and (e) Mo/Co ratio 5.

The synthesis of the potassium and hexamethonium salts of $[Mo_4(C_6H_5O_7)_2O_{11}]^{4-}$ and the structure of this anion were previously reported in Refs. [20,23], and are presented here in Fig. 3. However, those compounds could not be used for the preparation of bimetallic Co–Mo complexes and HDS catalysts. Ammonium salts of tetrameric anions have proven to be applicable for synthesis at certain pH intervals, and this has been extensively studied via

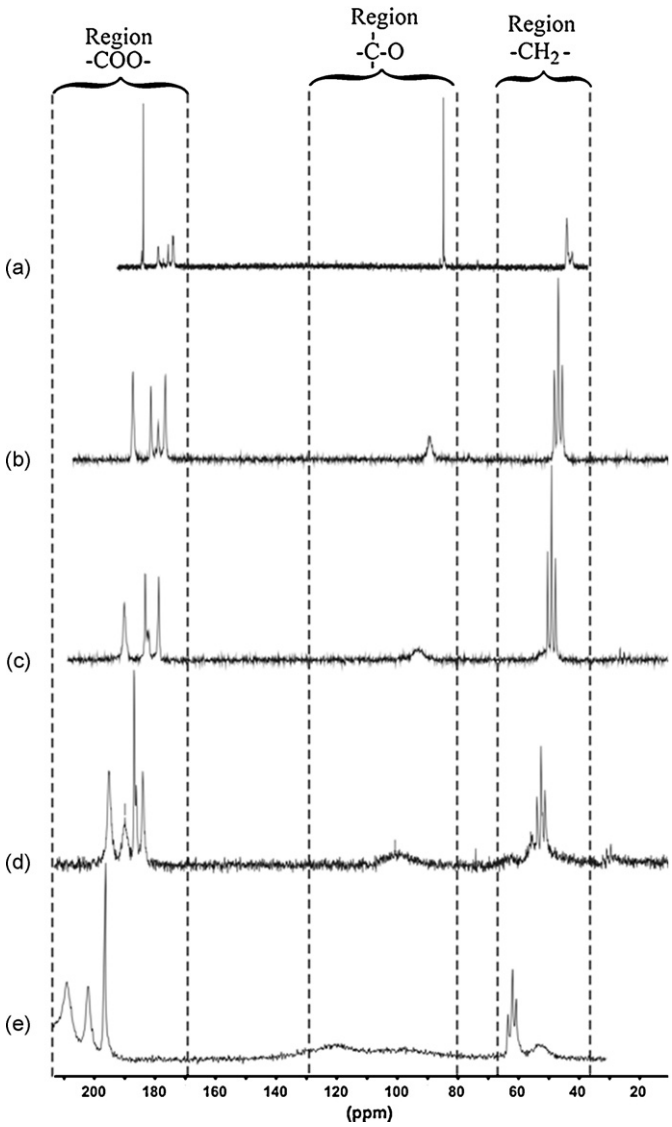

Fig. 2. ^{13}C NMR spectra of solutions. (Mo_4citr-solution) (a) and (Mo_4citr-solution) with different Co^{2+} addition: (b) Mo/Co ratio 40, (c) Mo/Co ratio 20, (d) Mo/Co ratio 10 and (e) Mo/Co ratio 5.

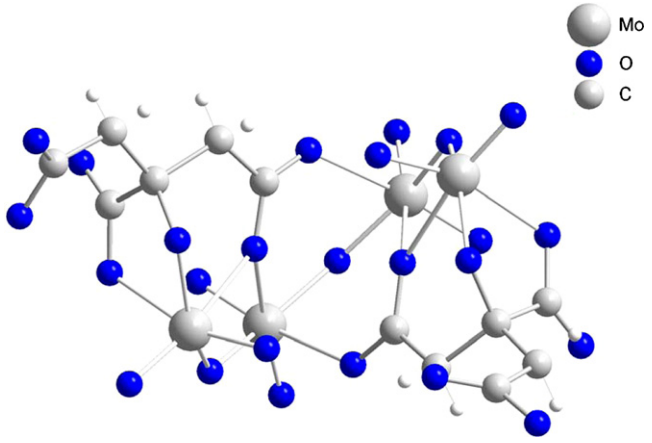

Fig. 3. The structure of the anion $[Mo_4(C_6H_5O_7)_2O_{11}]^{4-}$.

Raman spectroscopy in both the soluble form and when deposited on alumina, but there is a lack of structural information in these data [28]. Since the data on the structure of the anion in solution are of great importance, we have undertaken a study of the solutions by NMR spectroscopy of ^{95}Mo, ^{17}O and ^{13}C, which has provided considerable structural information about the polyoxometallates [29].

The tetrameric anion (Fig. 3) contains two types of Mo^{6+} ions (inner and outer ones), each having a corresponding terminal O atom (in Mo=O), bridged oxygen (Mo–O–Mo), and carboxyl oxygen atoms of three types, varying by their coordination to the molybdenum and carbon atoms of the citrate ligand. NMR spectra of (Mo_4citr-solution) (Table 1 and Figs. 1 and 2) revealed peaks for all of these species. The ^{95}Mo spectrum had two main peaks of almost the same intensity having chemical shifts intrinsic to the 6+ chemical state, with the upfield peak corresponding to the outer Mo atoms. The slight peak at δ = 76 ppm is due to impurities. The ^{17}O spectrum had peaks at δ = 865 ppm and 830 ppm that could be ascribed to terminal oxygen atoms bonded to outer and inner Mo atoms, respectively. The peak at δ = 371 ppm corresponds to bridged oxygen atoms, and the broad peak at δ = 260 ppm represents deprotonated oxygen in the carboxyl groups (protonated carboxyl oxygen has a peak at δ = 246 ppm that is observed in citric acid, but not in (Mo_4citr-solution)). The ^{17}O spectrum hardly indicated the possible coordination types of the carboxyl groups, but they may be easily distinguished from the ^{13}C spectra. Indeed, there are three distinct peaks in the range of 170–185 ppm, with the downfield (δ = 184.7 ppm) one corresponding to monodentate carboxyl species, the middle one to carboxyl species not coordinated to Mo, and the last (at δ = 173.9 ppm) representing carboxyl species bridging two Mo atoms (see Fig. 3). Other peaks in the ^{13}C spectra are $-CH_2-$ carbons and the central C atom in citrate.

In addition to the signals from the primary complex, the NMR spectra of (Mo_4citr-solution) had some extra peaks from other species whose content did not exceed 10%. Most likely, these species were ammonium salts of mono- and binuclear citrate complexes of molybdenum with structures similar to the potassium salts reported in [21,22]. Therefore, the NMR data showed that the prevalent species in (Mo_4citr-solution) is the $[Mo_4(C_6H_5O_7)_2O_{11}]^{4-}$ anion (Fig. 3).

The study of (Mo_4citr-solution AI) showed that its ^{13}C, ^{17}O and ^{95}Mo NMR spectra were very similar to those of (Mo_4citr-solution). The peak of ~600 Hz width at δ = 0.6 ppm in the ^{27}Al spectrum is probably due to the $Al(H_2O)_6^{3+}$ cation, although aluminum citrate complexes could not be ruled out. According to elemental analysis data, the concentration of aluminum does not exceed 2 g/dm^3, which is one order of magnitude lower than the content of molybdenum. Since the composition of Mo complexes in (Mo_4citr-solution AI) was the same as in (Mo_4citr-solution), we conclude that the structure of the primary $[Mo_4(C_6H_5O_7)_2O_{11}]^{4-}$ complex remains stable when in contact with alumina.

The addition of increasing amounts of paramagnetic Co^{2+} cations to (Mo_4citr-solution) was expected to cause shifting, broadening and eventually disappearance of NMR peaks, with the signals originating from the atoms directly coordinated to cobalt atoms being affected at first. In the ^{95}Mo spectra, a cobalt concentration increase caused monotonic peak broadening for both types of Mo atoms, with the upfield line (relating to the outer molybdenum atoms) having a relatively larger width. For the sample with Mo/Co = 2, the signal was so weak (comparable with the noise level) that it was difficult to accurately determine the position of the peak.

Concerning the ^{17}O spectra, the addition of cobalt mainly affected the signal from the carboxyl oxygen atoms and terminal oxygen atoms bonded to outer Mo atoms, while those bonded to inner Mo atoms and bridging oxygen (Mo–O–Mo) were less sensitive to cobalt (Fig. 1). Similar to the ^{95}Mo spectra, the total disappearance of ^{17}O signals occurred in the sample with Mo/Co = 2.

The ^{13}C spectra showed the most pronounced broadening for the peak related to the central atom of the citrate ligand that is close to the outer Mo atom (Fig. 2). Three types of carboxyl groups demonstrated the different broadening behavior; the width of the upfield peak of the bridged carboxyl group changed slightly, while both carboxyl groups coordinated to the outer Mo atoms and the carboxyl groups that were not coordinated to Mo showed very strong broadening. Thus, the NMR data indicated the formation of the labile complex $[Mo_4(C_6H_5O_7)_2O_{11}]^{4-}$ with Co^{2+} cations. Most likely, cobalt coordinates with the tetrameric anion via the terminal oxygen atom bonded to the outer molybdenum atom via the two types of carboxyl groups, one that is not coordinated with Mo and the other monodentate carboxyl group coordinated to the outer Mo via the oxygen atom bonded to the central carbon atom of the citrate ligand. The proposed structure of this bimetallic complex is presented in Fig. 4.

3.2. FTIR and Raman spectroscopy

FTIR and Raman data are presented in Tables 2 and 3, and the spectra are shown in Figs. 5 and 6. The infrared spectrum of the (Mo_4citr-solid) sample was very similar to the spectrum of the potassium salt of $[Mo_4(C_6H_5O_7)_2O_{11}]^{4-}$ [20], the structure of which is presented in Fig. 3. The bands at 1720–1330 cm^{-1} were assigned to valence vibrations of the carboxyl groups [30]. According to the structural data [20,23], the $[Mo_4(C_6H_5O_7)_2O_{11}]^{4-}$ anion has citrate ligands that contain three non-equivalent carboxylic groups; one is non-bonded and non-dissociated (characterized in our spec-

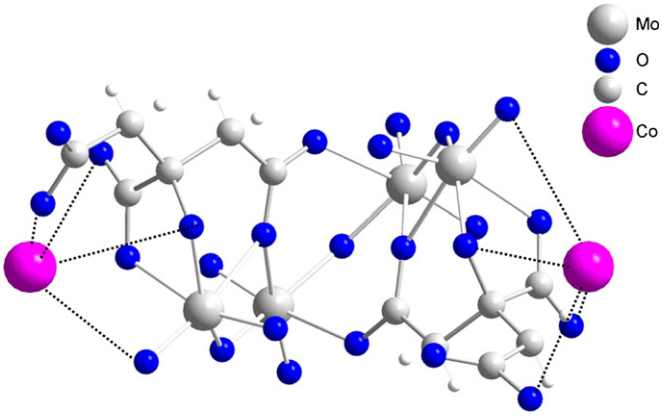

Fig. 4. Tentative structure of the bimetallic complex $Co_2[Mo_4(C_6H_5O_7)_2O_{11}]$.

Table 2
IR spectra and frequencies assignment of (Mo_4citr) and (Co_2Mo_4citr) complexes.

Assignment [20–22,30]	(Mo_4citr-solid)	(Mo_4citr-solution)	(Mo_4citr/Al_2O_3)	(Co_2Mo_4citr-solid)	(Co_2Mo_4citr-solution)	(Co_2Mo_4citr/ Al_2O_3)
ν(C=O) citr[a]	1721	1719	–	–	–	–
ν(C=O) acet[b]	–	–	–	1715	1712	–
ν_{as}(COO)[c]	1618, 1582	1623, 1588	1617, 1593	1621, 1587, 1554	1615, 1585, 1562	1591
ν_{as}(COO)[d]	1425, 1400	1450, 1422	1463, 1402	1433, 1402	1458, 1415	1437, 1404
ν(C–O) citr[e]	1230	1233	–	–	–	–
ν(C–O) acet[f]	–	–	–	1290, 1260	1292, 1269	–
Skeletal citrate	1181, 1147	1188, 1152	1183, 1156	1186, 1150	1186, 1153	1184, 1153
ν(C–O) alcohol	1081, 1072	1079, 1072	1081, 1074	1075	1079, 1070	1080
$\rho(CH_3)$ acet	–	–	–	1022	1019	–
ν(Mo=O)	943, 936, 924, 890, 884, 856, 848	943, 936, 923, 907, 892, 860	941, 931, 918, 906, 892, 861	932, 917, 905, 891, 859	936, 921, 909, 895, 862	932, 919, 902, 893, 862
ν(Mo–O–Mo)	795, 734, 710, 682, 641, 606	800, 736, 712, 683, 637, 612	802, 742, 709, 692, 661, 622	793, 738, 709, 688, 640, 615	800, 739, 714, 689, 641, 618	800, 739, 706, 683, 628, 623
δ(OMoO)	542, 518	544, 519	536, 514	548, 521	543, 521	537, 510

[a] ν(C=O) of citrate.
[b] ν(C=O) of acetic acid.
[c] Overlapped with $\delta(H_2O)$.
[d] Overlapped with $\delta_{as}(NH_4)$.
[e] ν(C–O) of citrate.
[f] ν(C–O) of acetic acid.

Table 3
Raman spectra and frequencies assignment of (Mo_4citr) and (Co_2Mo_4citr) complexes.

Assignment [22,24]	(Mo_4citr-solid)	(Mo_4citr-solution)	(Mo_4citr/Al_2O_3)	(Co_2Mo_4citr-solid)	(Co_2Mo_4citr-solution)	(Co_2Mo_4citr/Al_2O_3)
ν(Mo=O)	940, 922, 904, 896, 847	945, 901, 861	943, 899, 861	943, 896, 861	944, 898, 864	943, 900, 861
ν(Mo–O–Mo)	389, 376, 343	384, 374, 343	389, 373, 346	390, 374, 344	388, 372, 346	390, 378, 348
ν(O–Mo–O)	249, 214	249, 209	253, 212	250, 211	254, 210	251, 212

tra at 1721 and 1230 cm^{-1} for ν(C=O) and ν(C–O), respectively), one is coordinated to molybdenum in a monodentate fashion and the last is bridged to Mo. The corresponding vibration modes have positions at 1618 and 1582 (ν_{as}(COO)) and 1425 and 1400 cm^{-1} (ν_s(COO)), respectively. The latter bands were overlapping with the $\delta_{as}(NH_4^+)$ band. The valence stretching of ammonium also had a band at 3150 cm^{-1} (not shown in Fig. 5). The bands at 960–800 and 750–520 cm^{-1} were due to valence oscillations of the MoO_2 and Mo–O–Mo moieties. The most intense lines in the Raman spectrum were assigned to valence oscillations and deformation of the MoO_2 fragments (Fig. 6).

FTIR and Raman spectra for the (Mo_4citr-solution) sample did not noticeably differ from those for the (Mo_4citr-solid) sample. There were minor shifts in the vibrational frequencies, changes of relative signal intensities and broadening of some bands in the IR and lines in the Raman spectra.

Conversely, the IR spectrum of (Mo_4citr/Al_2O_3) was substantially different from the spectra of either the (Mo_4citr-solid) or the (Mo_4citr-solution) samples (Fig. 5). Thus, the vibrational bands of the protonated carboxylic groups were completely absent in the spectrum of the supported sample, most likely due to coordination of those groups to the aluminum atoms of the support. The spectra of the other carboxyl groups and of the MoO_2 fragments were changed as well. It was rather difficult to investigate the changes of the Mo–O–Mo spectra in the solution, solid and supported samples because these bands were fully overlapped with more intense bands from the support. However, the similarity of the Raman spectra for all three samples (((Mo_4citr-solid), (Mo_4citr-solution) and

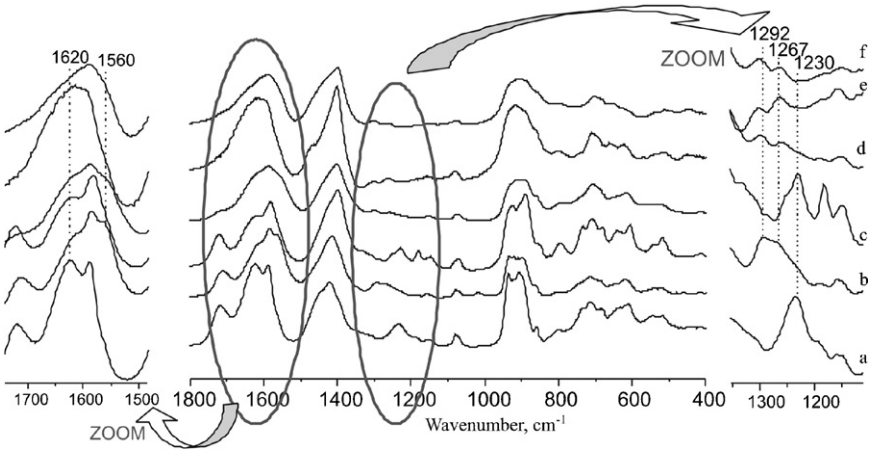

Fig. 5. FTIR spectra in a full range and scaled up regions of 1490–1730 cm^{-1}, 1110–1350 full cm^{-1} for the Mo and Co–Mo complexes: (Mo_4citr-solution) (a), (Co_2Mo_4citr-solution) (b), (Mo_4citr–solid) (c), (Co_2Mo_4citr-solid) (d), (Mo_4citr/Al_2O_3) (e) and (Co_2Mo_4citr/Al_2O_3) (f).

(Mo_4citr/Al_2O_3)) indicated that the tetranuclear structure was not changed after the deposition (Fig. 6). Hence, our data conformed to the results reported in [24,28], where Raman spectroscopy data confirmed the stability of the $[Mo_4O_{11}(C_6H_5O_6)_2]^{4-}$ structure after deposition on alumina.

The interaction of the $[Mo_4O_{11}(C_6H_5O_6)_2]^{4-}$ anion with Co^{2+} cations resulted in more apparent spectral changes. We propose that the differences in the positions and intensities of absorbance bands listed below are due to the coordination of cobalt to tetrameric anions. There are some references reporting tetrameric anion complexes with K^+ and $[(CH_3)_3N(CH_2)_6N(CH_3)_3]^{2+}$ [20–23], but any information regarding the effect of either the cation nature or its location in the IR is absent. The structural data indicated that potassium atoms or nitrogen atoms of $[(CH_3)_3N(CH_2)_6N(CH_3)_3]^{2+}$ coordinated to terminal oxygen atoms and oxygen atoms of carboxyl groups bonded with outer Mo atoms [20,23]. If, presumably, Co^{2+} cations occupy the same positions, then the corresponding spectra should be changed.

Indeed, our experimental data (Fig. 5 and Table 2) showed that the addition of cobalt acetate to (Mo_4citr-solution) gave (Co_2Mo_4citr-solution) (with an atomic Mo/Co ration of 2), and drastically altered the spectrum of the ν(C–O) spectral region for the non-dissociated carboxyl groups, specifically, the 1230 cm^{-1} band vanished and two intense bands at 1269 and 1292 cm^{-1} appeared. The position of the ν(C=O) band was shifted from 1719 to 1712 cm^{-1}. The disappearance of the 1230 cm^{-1} band gave clear evidence that cobalt atoms are coordinated to the free carboxyl groups. In this case, non-dissociated carboxyl groups do not belong to the citrate ligand, but rather to the acetic acid that is produced in the course of the reaction. Thus, the 1019 cm^{-1} band that appeared in the spectrum was the deformation vibrational mode of the methyl moiety of acetic acid. Additionally, strong changes were observed in the ν_{as}(COO) vibrational spectra of the carboxyl groups of the citrate ligand coordinated with molybdenum, i.e. the relative intensity of the 1620 cm^{-1} band decreased noticeably and a new band at 1562 cm^{-1} appeared. The 1620 cm^{-1} band could be attributed to asymmetric valence stretching of the monodentate COO groups of the citrate ligands. Both the attenuation of this signal and the appearance of the new ν_{as}(COO) band at a lower frequency could be explained by the interaction between the monodentate group of the citrate ligand and the Co^{2+} ion in such way that this group coordinates and thus has a lower ν_{as}(COO) vibrational frequency of ~1560 cm^{-1}. There were also visible changes in the spectral region of the valence vibrations of the MoO_2 fragments that were mainly significant alterations of the relative intensities and, to a lesser extent, changes in the shifts of these bands. This effect is most likely due to the interaction of Co^{2+} ions with the terminal oxygen atoms of this fragment. The spectra of both the Mo–O–Mo moiety and the bridged carboxyl group remained almost unchanged. The major difference between the (Co_2Mo_4citr-solid) IR spectrum and that of (Co_2Mo_4citr-solution) was the much lower intensity of the acetic acid signal. Therefore, one could conclude that the structure of the $[Mo_4(C_6H_5O_7)_2O_{11}]^{4-}$ anion in solution and in the solid state are the same. The IR spectrum of the supported complex had the larger absorbance band width.

Raman spectra of Co-containing samples differed from the spectra of samples without cobalt, mainly in the region of the valence vibrations of the MoO_2 fragment. As in the IR spectra, the most prominent distinction was in the intensities rather than in the positions of the peaks.

Thus, the addition of cobalt acetate to (Mo_4citr-solution) affected the positions and intensities of absorbance bands corresponding to valence vibrations of the carboxyl groups and MoO_2 fragments, whereas a majority of the other bands, including the vibrations of bridged carboxyl groups and Mo–O–Mo species, remained unchanged.

All alterations in the spectra induced by the addition of cobalt could be most simply explained by the presumption that Co^{2+} cations are coordinated to $[Mo_4(C_6H_5O_6)_2O_{11}]^{4-}$ anions at exactly the same positions that K^+ or $[(CH_3)_3N(CH_2)_6N(CH_3)_3]^{2+}$ would coordinate [20,23], specifically toward the oxygen atoms of carboxyl groups bonded to single Mo atoms, oxygen atoms of the unoccupied carboxyl groups and terminal oxygen atoms, while the structure of the tetrameric anion would remain intact.

As followed from Table 2, the main bands in the IR spectrum of (Mo_4citr/Al_2O_3) sample corresponds to the basic bands of (Mo_4citr-solution), the main bands in the IR spectrum of (Co_2Mo_4citr/Al_2O_3) sample is identical to that in bimetallic complex solution spectrum, analogically for Raman spectra of the studied solutions and supported catalysts (Table 3). The good

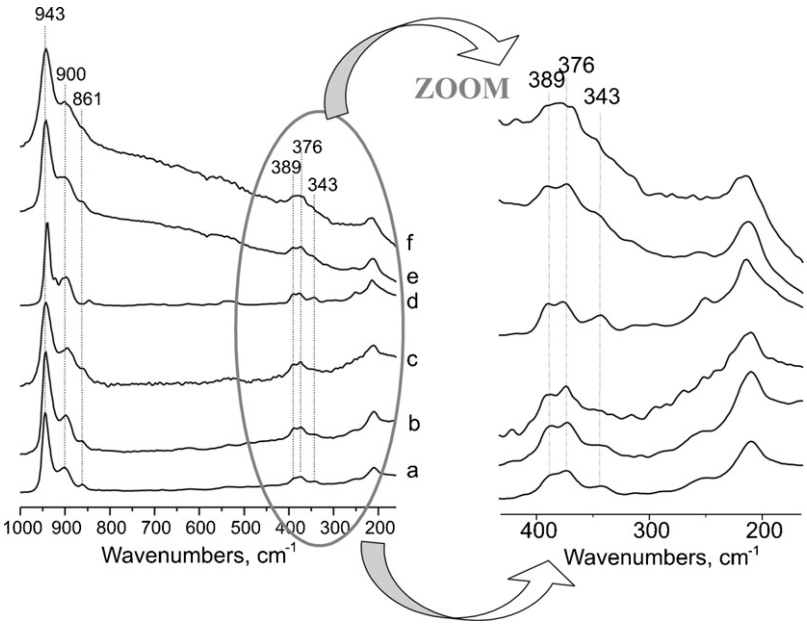

Fig. 6. Laser Raman spectra in the region of 160–1000 cm^{-1} and scaled up region of 180–600 cm^{-1} for the Mo and Co–Mo complexes: (Mo_4citr–solution) (a), (Co_2Mo_4citr-solution) (b), (Mo_4citr-solid) (c), (Co_2Mo_4citr-solid) (d), (Mo_4citr/Al_2O_3) (e) and (Co_2Mo_4citr/Al_2O_3) (f).

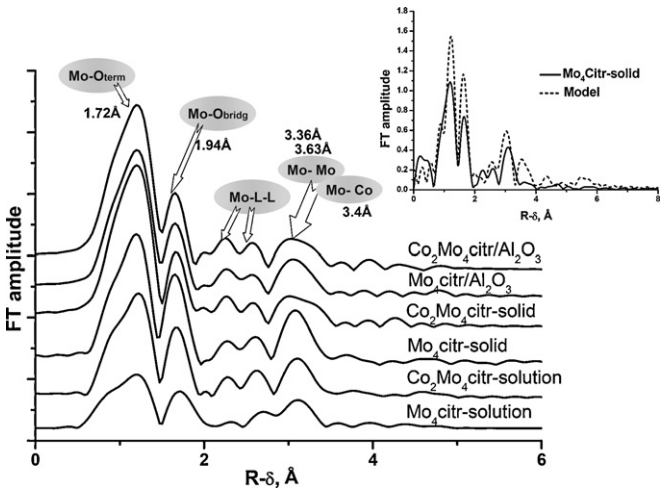

Fig. 7. Fourier transform of molybdenum K-edge EXAFS spectra for the Mo and Co–Mo complexes. The model and experimental curves (Mo_4citr-solid) are shown in the right corner.

conformity in both the positions and intensities of the IR and Raman spectra for the (Co_2Mo_4citr-solid), (Co_2Mo_4citr-solution) and (Co_2Mo_4citr/Al_2O_3) samples supports the constancy of Co coordination to Mo-containing anions, even at the support surface, i.e. the interaction of bimetallic Co–Mo compounds with alumina does not lead to its decomposition.

3.3. Data from XAS spectroscopy

The radial distribution functions (RDF) of atoms around Mo and Co are presented in Figs. 7 and 8. RDF curves of Mo local surroundings for all of the samples, whether in the solution, solid or supported state, regardless of the presence or absence of cobalt, have two maxima in the length range of ligand bonds that correspond to Mo–O distances of 1.72 and 1.94 Å in simulated curves. The former peak gives the average distance of Mo to terminal oxygen atoms, and the latter value is the mean distance from Mo to bridged O atoms of hydroxyl groups and from Mo to oxygen atoms of citrate ligands. The peaks located within 2–3 Å range corresponds to the distances from molybdenum to other atoms in citrate ligands and to oxygen surrounding of neighbor molybdenum atom, the peak

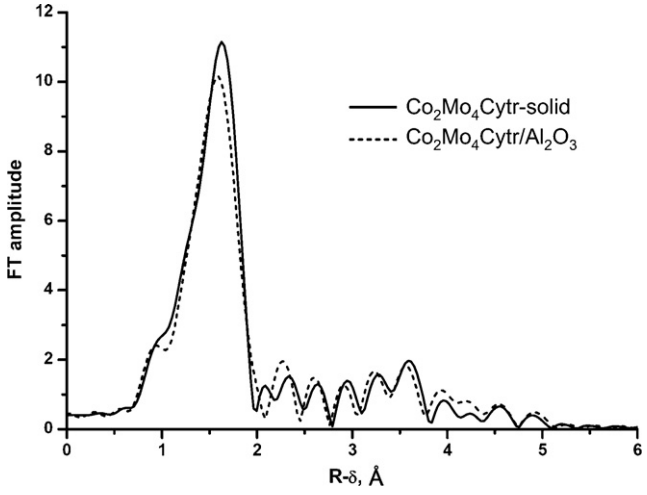

Fig. 8. Fourier transform of cobalt K-edge EXAFS spectra for the bimetallic complex in solid state and alumina-supported form.

denoted as Mo–L–L in Fig. 7. Since any studied sample contains 2, 3 or 4 different types of Mo atoms, each having its own specific ligand, the modeling is capable of obtaining the effective coordination numbers, and the results of such calculations were omitted here. One should mention the broadening of all of the peaks for the solution samples, obviously due to the higher amplitude of thermal oscillations in solution as compared to the solid and supported samples, which are present as Debye–Waller factors in the EXAFS spectra.

RDF curves for the samples without cobalt had a very similar set of maxima in the range of R-δ>2 Å (Fig. 7). Experimental and fitted RDF curves are presented in Fig. 7. Our results are in good agreement with the reported structure of the potassium salt [20] where Mo atoms are coupled in pairs with a Mo–Mo distance of 3.36 Å and the neighboring pairs form a single bond 3.62 Å in length. The intense peak at 3.36 Å corresponds to Mo–Mo spacing, and the maxima within the 1.94 and 3.36 Å interval should be assigned to the distances from Mo to other atoms in the citrate ligand. The cardinal distinction of ammonium salts synthesized by us when compared with the reported potassium salts is that the experimental RDF curve does not show the peak of the second Mo–Mo distance that is rather evident in the model curve. We suppose that our complexes are hydrated to a greater extent than $K_4[(MoO_2)_4O_3(citr)_2]\cdot 6H_2O$, and thus have a more distorted structure. The comparison of RDF curves for the (Mo_4citr-solid) and (Mo_4citr/Al_2O_3) samples showed some dispersion of distance values and attenuation of the signal corresponding to the Mo-Mo distance. Again, both the different extent of hydration and the interaction with the support are the main reasons for the cationic lattice deformation that occurs in the course of impregnation of alumina with the complex.

Since the experimental data for the samples without cobalt are in good agreement with the known structure of the tetrameric anion, we conclude that in the ammonium salt discussed here, the $[Mo_4(C_6H_5O_7)_2O_{11}]^{4-}$ anion has the structure presented in Fig. 3, probably with some minor distortions. Moreover, this structure remains almost unchanged in solution, the solid state and the alumina-supported form.

The reaction between $[Mo_4(C_6H_5O_7)_2O_{11}]^{4-}$ and Co acetate drastically changed the data of the XAS spectroscopy of molybdenum (Fig. 9a and b). First, XANES Mo K-edge spectra for the (Co_2Mo_4citr-solid) sample demonstrated a curve shift of 2 eV to higher energies as compared with (Mo_4citr-solid) (Fig. 9a). The same effect was observed when $[Mo_4(C_6H_5O_7)_2O_{11}]^{4-}$ interacted with an alumina surface; the shifts of curves recorded for the (Mo_4citr-solid) and (Mo_4citr/Al_2O_3) samples were also ~2 eV (Fig. 9b). Thus, the interaction of the tetrameric anion with either Co^{2+} cations or the alumina surface, regardless of the reactant nature, leads to the same changes in the Mo charge state. One should note that according to a comparison of the (Co_2Mo_4citr-solid) and (Co_2Mo_4citr/Al_2O_3) XANES spectra, the deposition of bimetallic Co–Mo to the alumina surface does not change the Mo charge state.

RDF Mo K-edge curves for the samples with and without cobalt were almost identical in the R-δ<3 Å range (Fig. 7). Regardless of the aggregate state of the samples, the bimetallic complexes differed from the Mo ones by having two maxima for the Mo-metal distances, in the range of 3.3–3.7 Å. The maximum at 3.36 Å is certainly for Mo–Mo, but on the basis of Mo K-edge spectra, it is hardly distinct from the second distance between Mo–Mo (3.72 Å) and Mo–Co (3.41 Å); both variants have a discrepancy factor of 1%. However, we suppose that this second maximum originates from Mo–Co spacing, since in the RDF curves for (Co_2Mo_4citr-solid) and (Co_2Mo_4citr/Al_2O_3), we noticed two other peaks around R-δ>3.8 Å. The corresponding distances could not be assigned unambiguously, but just the appearance of these peaks indicated that the bimetallic compound is more rigid than the Mo complex. Thus, cobalt has

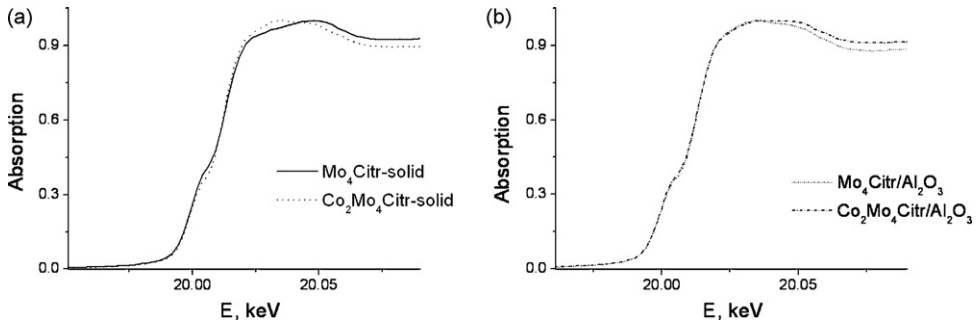

Fig. 9. XANES spectra of solid (Mo_4citr-solid) and (Co_2Mo_4citr-solid) samples (a), and supported (Mo_4citr/Al_2O_3) and (Co_2Mo_4citr/Al_2O_3) catalysts (b).

been proven to interact with the $[Mo_4(C_6H_5O_7)_2O_{11}]^{4-}$ anion and distort its cationic lattice. Most likely, Co is coordinated to terminal oxygen atoms and to carboxyl groups that are not bonded with molybdenum, as the resulting structure is the most rigid in this case.

The RDF Co K-edge curves (Fig. 8) for the (Co_2Mo_4citr-solid) and (Co_2Mo_4citr/Al_2O_3) samples were almost identical, and the most intense peak corresponded to a Co–O distance of 2.06 Å, with a coordination number of 4. This distance, within the experimental error (±0.02 Å), agrees with the reference data on hydrated cobalt chloride, nitrate and acetate salts [31]. However, in the R-δ>2 Å region, the acquired RDF curves exhibited the maxima related to at least six coordination spheres, whereas the RDF curve for monomeric Co acetate should have three or fewer coordination spheres for the more distant carbon atoms of the ligand. Therefore, our results do not absolutely conform to the data reported in Ref. [31] or with the RDF curves for bulk cobalt acetate ($Co(CH_3COO)_2{\cdot}4H_2O$) presented in Ref. [32]. Thus, we conclude that the RDF curves of the (Co_2Mo_4citr-solid) and (Co_2Mo_4citr/Al_2O_3) samples represent the products of the reaction between Co acetate and the $[Mo_4(C_6H_5O_7)_2O_{11}]^{4-}$ anion.

Summarizing the results of XAS spectroscopy gives strong evidence of bimetallic compound formation with cobalt coordinated to the $[Mo_4(C_6H_5O_7)_2O_{11}]^{4-}$ anion and a Co–Mo distance of 3.41 Å, as proven in both the Co K-edge and Mo K-edge spectra. The absence of a noticeable difference in RDF curves for the discussed bimetallic complex in the (Co_2Mo_4citr-solution), (Co_2Mo_4citr-solid) and (Co_2Mo_4citr/Al_2O_3) samples, along with the absolute identity of the XANES spectra for the (Co_2Mo_4citr-solid) and (Co_2Mo_4citr/Al_2O_3) samples, unambiguously indicated that the structure of the bimetallic compound remained the same for the complex in solution, in the solid state and on the alumina surface.

3.4. Catalyst testing in the HDS reaction

The results of the testing of the (Co_2Mo_4citr/Al_2O_3) sample in the HDS of straight run diesel fuel are presented in Fig. 10. The chosen testing conditions are attainable in industrial apparatuses for the HDS of diesels at most Russian and worldwide petrochemical plants, and a typical Russian straight run gas oil fraction was used as the feedstock [33–35]. Similar conditions for the HDS process were employed in another paper [36], where catalysts enabling the production of ~10 ppm sulfur fuels were reported.According to Ref. [35] over commercial catalysts TK-554, 424 T @, 448 T @ (Ø1, 3) and 448 T @ (Ø2, 5) the residual sulfur content are 400, 1800, 400, 750 ppm, respectively, at LHSV of 4 h^{-1} and temperature of 345 °C. For Russian commercial catalysts GKD-300 and GM-85 (Co) the residual sulfur content is much higher. Over (Co_2Mo_4citr/Al_2O_3) catalyst at the above-specified conditions the residual sulfur content is 310 ppm (Fig. 10b).To obtain ultralow-sulfur diesel the feed flow varied in the range of 1.3–2.5 h^{-1} [18,33–36]. The (Co_2Mo_4citr/Al_2O_3) catalyst provides obtaining of diesel fuel with sulfur content in the product of 50 and 10 ppm at temperatures of 340 and 360 °C, respectively (Fig. 10a), the rest process parameters are weight flow rate of 2 h^{-1}, pressure of 3.5 MPa and H_2/feed volume ratio of 300 Nm^3/m^3. It is reported that diesel fuel with sulfur content of 10 ppm over commercial C-606A catalyst was obtained at 340–345 °C [36], but in referred paper more stringent conditions were used, flow rate of 1.5 h^{-1} and pressure of 4.9 MPa. Over KF-757 catalyst the diesel fuel with sulfur content laying in the range from 8 to 31 ppm was obtained at an average temperature of 353 °C, pressure of 3.28 MPa and H_2/feed volume ratio 400 Nm^3/m^3 [35].

Thus, the comparison of our results (Fig. 10) with the trial results of the prospective ultra-deep HDS catalyst for ULSD production [36] and with the testing results for the commercial catalysts of

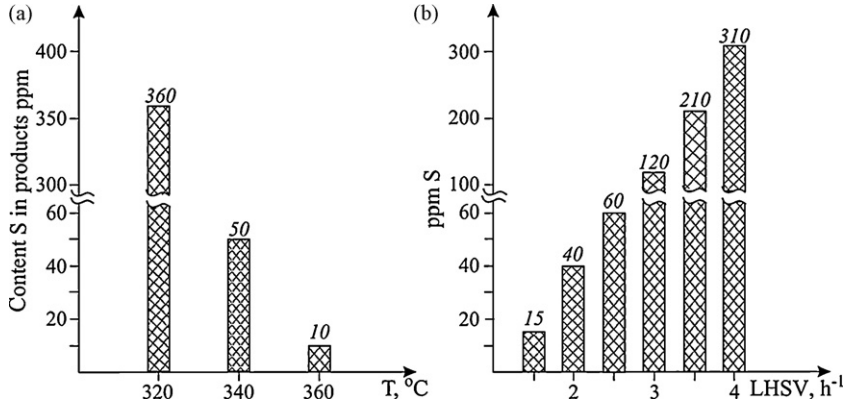

Fig. 10. The results of (Co_2Mo_4citr/Al_2O_3) hydrotreating activity test obtained at 3.5 MPa, H_2/feed volume ratio 300: (a) LHSV = 2 h^{-1}, T = 320–360 °C and (b) T = 345 °C, LHSV = 1.5–4 h^{-1}.

the leading worldwide manufacturers [35] with a feedstock with similar properties revealed that our (Co_2Mo_4citr/Al_2O_3) catalyst is highly competitive with the referenced samples, and is capable of producing diesel with <50 ppm sulfur and <10 ppm sulfur.

4. Discussion

This NMR study of (Mo_4citr-solution) has shown that dissolving ammonium heptamolybdate in an aqueous citrate acid solution with a pH value between 1.5 and 3.5 leads mainly to the formation of the ammonium salt of the tetrameric $[Mo_4(C_6H_5O_7)_2O_{11}]^{4-}$ anion, with the structure presented in Fig. 3. The solute state of this complex was characterized by FTIR, Raman and XAS spectroscopy, and the obtained results allowed us to conclude that the structure of the $[Mo_4(C_6H_5O_7)_2O_{11}]^{4-}$ anion remained unchanged after precipitation (Mo_4citr-solid sample) and after impregnation of alumina (Mo_4citr/Al_2O_3 sample), in full accordance with reference data [24,28].

Gradual addition of increasing amounts of cobalt acetate to a (Mo_4citr-solution) sample affected the peaks in the NMR spectra of certain atoms due to the coordination of paramagnetic Co^{2+} cations to specific fragments of the $[Mo_4(C_6H_5O_7)_2O_{11}]^{4-}$ anion. The coordination occurs via bonding with outer Mo atoms via oxygen atoms of monodentate carboxyl groups (see Fig. 3), with the other carboxyl group not coordinated to Mo and with oxygen atoms bonded to the central carbon atom of the citrate ligand. We suppose that the peak broadening to the point of total disappearance both in the ^{95}Mo and ^{17}O spectra at a Mo/Co atomic ratio of 2 is an intrinsic peculiarity for a bimetallic compound with this stoichiometry.

FTIR, Raman and XAS spectroscopy data also confirmed the formation of a bimetallic Co–Mo complex (with the structure presented in Fig. 4) in solution. Moreover, these methods allowed us to monitor the structure of the synthesized compound in the solid state and in the alumina-supported form. The collected results indicated that deposition to the alumina surface did not damage the structure of the primary tetranuclear $[Mo_4(C_6H_5O_7)_2O_{11}]^{4-}$ anion and its coordination with two Co^{2+} cations. The proximity of the cobalt and molybdenum atoms (3.41 Å) in the discussed complex facilitates the formation of uniform bimetallic sulfide compounds (probably of the Co–Mo–S Type II phase [17,18]) after catalyst sulfidation. It should be noted that as in Ref. [36], our synthesis does not include high-temperature calcination prior to the sulfidation stage to save local environment of Co and Mo atoms and coordination of Co atoms towards Mo-containing species and to avoid the formation of catalytically inactive Co compounds with alumina or sulfur [12]. The sulfidation process for the catalysts prepared using citric acid was comprehensively studied [37,38] and the obtained results agree with discussed assumption that the preparation of the active catalyst needs the sulfidation under conditions providing the close proximity of Co and Mo atoms.

Thus, the implementation of both the proper synthesis of the bimetallic Co–Mo compound in solution and evaluation of the optimal conditions for its impregnation of alumina with the compound and drying (so that the structure of bimetallic complex remains intact) resulted in the preparation of a catalyst capable of producing diesel with <50 ppm sulfur and <10 ppm sulfur.

5. Conclusion

In this paper, we extensively studied a deep HDS catalyst for ULSD production, prepared via the synthesis of a bimetallic Co–Mo complex in solution with a Mo/Co ratio typical of commercial HDS catalysts. In the first stage, the ammonium salt of the tetrameric anion $[Mo_4(C_6H_5O_7)_2O_{11}]^{4-}$ was synthesized in solution. Then, two Co^{2+} cations were coordinated to this anion, and the structure of the prepared compound was elucidated. The cobalt was shown to coordinate via the terminal oxygen atom, the oxygen atom bonded with the central atom of the citrate ligand and two carboxyl groups. After impregnation of alumina and drying at room temperature, the structure of the obtained surface compound was the same as for the bimetallic complex synthesized in solution. After sulfidation, the prepared catalyst demonstrated very high activity in the HDS production of ultraclean diesel fuel.

Acknowledgments

The authors are grateful to the Russian Foundation for Basic Research for financial support of their participation in the International Symposium on Catalysis for Ultra Clean Fuels, Dalian, China, July 21–24, 2008 (project No 08-03-08283-z).

References

[1] P. Blanchard, C. Lamonier, A. Griboval, E. Payen, Appl. Catal. A: Gen. 322 (2007) 33–45.
[2] C. Lamonier, C. Martin, J. Mazurelle, V. Harle, D. Guillaume, E. Payen, Appl. Catal. B: Environ. 70 (2007) 548–556.
[3] J. Mazurelle, C. Lamonier, C. Lancelot, E. Payen, C. Pichon, D. Guillaume, Catal. Today 130 (2008) 41–49.
[4] C.I. Cabello, F.M. Cabrerizo, A. Alvarez, H.J. Thomas, J. Mol. Catal. A: Chem. 186 (2002) 89–100.
[5] C.I. Cabello, I.L. Botto, H.J. Thomas, Appl. Catal. A: Gen. 197 (2000) 79–86.
[6] J.A. Bergwerff, T. Visser, B.M. Weckhuysen, Catal. Today 130 (2008) 117–125.
[7] A. Griboval, P. Blanchard, E. Payen, M. Fournier, J.L. Dubois, Catal. Today 45 (1998) 277–283.
[8] R.R. Chianelli, M. Daage, M.J. Ledoux, Adv. Catal. 40 (1994) 177–232.
[9] C. Leyva, J. Ancheyta, M.S. Rana, G. Marroquin, Fuel 86 (2007) 1232–1239.
[10] I. Pettiti, I.L. Botto, C.I. Cabello, S. Colonna, M. Faticanti, G. Minelli, et al., Appl. Catal. A: Gen. 220 (2001) 113–121.
[11] C. Martin, C. Lamonier, M. Fournier, O. Mentre, V. Harle, D. Guillaume, et al., Inorg. Chem. 43 (15) (2004) 4636–4644.
[12] J.V. Lauritsen, J. Kibsgaard, G.H. Olesen, P.G. Moses, B. Hinnemann, S. Helveg, et al., J. Catal. 249 (2007) 220–333.
[13] J.A. Bergwerff, L.G.A. van de Water, A.A. Lysova, I.V. Koptyug, T. Visser, K.P. de Jong, et al., Stud. Surf. Sci. Catal. 162 (2006) 175–186.
[14] D. Nicosia, R. Prins, J. Catal. 234 (2005) 414–420.
[15] J.A.R. Van Veen, P.A.J.M. Hendriks, R.R. Andrea, E.J.G.M. Romers, A.E. Wilson, J. Phys. Chem. 94 (1990) 5282–5285.
[16] J. Bergwerff, L. van de Water, T. Visser, K. de Jong, B. Weckhuysen, Proc. Seventh European Congress on Catalysis, 28 August–1 September, Sofia, Bulgaria, 2005, pp. 01–08.
[17] R. Candia, O. Soerensen, J. Villadsen, N.-Y. Topsoe, B.S. Clausen, H. Topsoe, Bull. Soc. Chim. Belg. 93 (1984) 763–765.
[18] S. Eijsbouts, L.C.A. van den Oetelaar, R.R. van Ruijenbroek, J. Catal. 229 (2005) 352–364.
[19] A.S. Noskov, G.A. Bukhtiyarova, A.S. Ivanova, O.V. Klimov, A.V. Pashigreva, Ya.M. Polunkin, et al., Proc. 7th Russian Oil Gas and Energy International Forum, 10–12 April, St. Petersburg, 2007, pp. 245–248.
[20] N.W. Alcock, M. Dudek, R. Grybos, E. Hodorowicz, A. Kanas, A. Samotus, J. Chem. Soc., Dalton Trans. (1990) 707–711.
[21] Z.-H. Zhou, H.-L. Wan, K.-R. Tsai, Inorg. Chem. 39 (2000) 59–64.
[22] A. Samotus, A. Kanas, M. Dudek, R. Grybos, E. Hodorowicz, Trans. Met. Chem. 16 (1991) 495–499.
[23] L.R. Nassimbeni, M.L. Niven, J.J. Cruywagen, J.B.B. Heyns, J. Cryst. Spectrosc. Res. 17 (1987) 373–382.
[24] J.A. Bergwerff, T. Visser, B.R.G. Leliveld, B.D. Rossenaar, K.P. de Jong, B.M. Weckhuysen, J. Am. Chem. Soc. 126 (2004) 14548–14556.
[25] D.I. Kochubey, EXAFS-spectroscopy of the catalysts, Science, Novosibirsk (1992).
[26] K.V. Klementev, J. Phys. D: Appl. Phys. 34 (2001) 209–217.
[27] J.J. Rehr, A.L. Ankudinov, Radiat. Phys. Chem. 70 (2004) 453–463.
[28] J.A. Bergwerff, M. Jansen, B.R.G. Leliveld, T. Visser, K.P. de Jong, B.M. Weckhuysen, J. Catal. 243 (2006) 292–302.
[29] M.A. Fedotov, R.I. Maksimovskaya, J. Struct. Chem. 47 (2006) 952–978.
[30] K. Nakamoto, Infrared and Raman Spectra of Inorganic and Coordination Compounds, New York, John Wiley and Sons, 1986.
[31] C.C. Harrison, X. Li, I. Hopkinson, S.E. Stratford, A. Guy Orpen, J. Chem. Soc. Faraday Trans. 89 (1993) 4115–4122.
[32] J.S. Girardon, A.S. Lermontov, L. Gengembre, P.A. Chernavskii, A. Griboval-Constant, A.Y. Khodakov, J. Catal. 230 (2005) 339–352.
[33] O.V. Klimov, A.V. Pashigreva, G.A. Bukhtiyarova, V.N. Kashkin, A.S. Noskov, Y.M. Polunkin, Catalysis in Industry, Special Release, 2008, pp. 6–13.
[34] A.V. Pashigreva, G.A. Bukhtiyarova, O.V. Klimov, A.S. Noskov, Ya.M. Polunkin, Neftepererabotka I neftekhimija 10 (2007) 19–23 [in Russian].

[35] V.G. Rassadin, O.V. Durov, G.G. Vasiljev, Chemistry Technology of Fuels and Oils, vol. 1, 2007, pp. 3–9.
[36] T. Fujikawa, H. Kimura, K. Kiriyama, K. Hagiwara, Catal. Today 111 (2006) 188–193.
[37] A.V. Pashigreva, G.A. Bukhtiyarova, O.V. Klimov, Yu.A. Chesalov, G.S. Litvak, A.S. Noskov, Catal Today 149 (2010) 19–27.
[38] G.A. Bukhtiyarova, O.V. Klimov, D.I. Kochubey, A.S. Noskov, A.V. Pashigreva, Nucl. Instrum. Methods Phys. Res. Sect. A 603 (2009) 119–121.